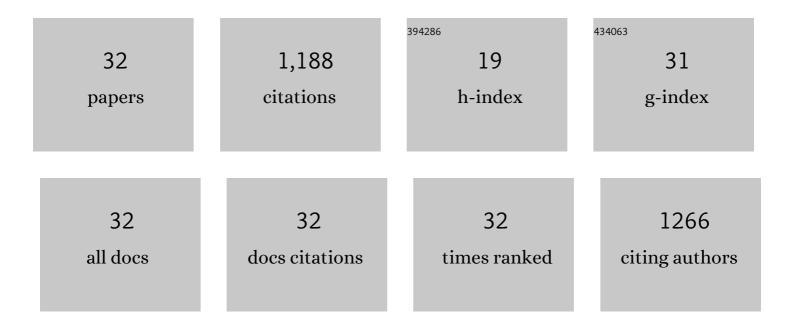
Lukas Keller

List of Publications by Year in descending order

Source: https://exaly.com/author-pdf/9561551/publications.pdf Version: 2024-02-01



LINNG KELLED

#	Article	IF	CITATIONS
1	3D pore microstructures and computer simulation: Effective permeabilities and capillary pressure during drainage in Opalinus Clay. Oil and Gas Science and Technology, 2021, 76, 44.	1.4	1
2	Petrophysical Properties of Opalinus Clay Drill Cores Determined from Med-XCT Images. Geotechnical and Geological Engineering, 2019, 37, 3507-3522.	0.8	8
3	Consolidated-undrained triaxial testing of Opalinus Clay: Results and method validation. Geomechanics for Energy and the Environment, 2018, 14, 16-28.	1.2	34
4	Imageâ€Based Upscaling of Permeability in Opalinus Clay. Journal of Geophysical Research: Solid Earth, 2018, 123, 285-295.	1.4	32
5	Understanding anisotropic mechanical properties of shales at different length scales: In situ micropillar compression combined with finite element calculations. Journal of Geophysical Research: Solid Earth, 2017, 122, 5945-5955.	1.4	16
6	Porosity anisotropy of Opalinus Clay: implications for the poroelastic behaviour. Geophysical Journal International, 2017, 208, 1443-1448.	1.0	7
7	Pore geometry effects on elastic properties of Opalinus Clay. Geophysics, 2016, 81, D543-D551.	1.4	5
8	Impact of sand content on solute diffusion in Opalinus Clay. Applied Clay Science, 2015, 112-113, 134-142.	2.6	16
9	Intergranular pore space evolution in MX80 bentonite during a long-term experiment. Applied Clay Science, 2015, 104, 150-159.	2.6	8
10	The Pore Structure of Compacted and Partly Saturated MX-80 Bentonite at Different Dry Densities. Clays and Clay Minerals, 2014, 62, 174-187.	0.6	24
11	On the Potential of Tomographic Methods when Applied to Compacted Crushed Rock Salt. Transport in Porous Media, 2014, 104, 607-620.	1.2	1
12	Characterization of multi-scale microstructural features in Opalinus Clay. Microporous and Mesoporous Materials, 2013, 170, 83-94.	2.2	152
13	Threeâ€dimensional pore structure and ion conductivity of porous ceramic diaphragms. AICHE Journal, 2013, 59, 1446-1457.	1.8	52
14	Redox cycling of Ni–YSZ anodes for solid oxide fuel cells: Influence of tortuosity, constriction and percolation factors on the effective transport properties. Journal of Power Sources, 2013, 242, 179-194.	4.0	59
15	Pore space relevant for gas permeability in Opalinus clay: Statistical analysis of homogeneity, percolation, and representative volume element. Journal of Geophysical Research: Solid Earth, 2013, 118, 2799-2812.	1.4	91
16	3D geometry and topology of pore pathways in Opalinus clay: Implications for mass transport. Applied Clay Science, 2011, 52, 85-95.	2.6	190
17	On the application of focused ion beam nanotomography in characterizing the 3D pore space geometry of Opalinus clay. Physics and Chemistry of the Earth, 2011, 36, 1539-1544.	1.2	75
18	The single-slip hypothesis revisited: Crystal-preferred orientations of sheared quartz aggregates with increasing strain in nature and numerical simulation. Journal of Structural Geology, 2011, 33, 1491-1500.	1.0	25

Lukas Keller

#	Article	IF	CITATIONS
19	The behavior of Mg, Fe, and Ni during the replacement of olivine by orthopyroxene: experiments relevant to mantle metasomatism. Mineralogy and Petrology, 2011, 103, 1-8.	0.4	10
20	Reaction rim growth inÂtheÂsystemÂMgO-Al2O3-SiO2 underÂuniaxialÂstress. Mineralogy and Petrology, 2010, 99, 263-277.	0.4	28
21	Enhancement of solid-state reaction rates by non-hydrostatic stress effects on polycrystalline diffusion kinetics. American Mineralogist, 2010, 95, 1399-1407.	0.9	27
22	Complex chemical zoning in eclogite facies garnet reaction rims: the role of grain boundary diffusion. Mineralogy and Petrology, 2009, 95, 303-313.	0.4	9
23	Asymmetrically zoned reaction rims: assessment of grain boundary diffusivities and growth rates related to natural diffusionâ€controlled mineral reactions. Journal of Metamorphic Geology, 2008, 26, 99-120.	1.6	32
24	Component mobility at 900°C and 18kbar from experimentally grown coronas in a natural gabbro. Geochimica Et Cosmochimica Acta, 2008, 72, 4307-4322.	1.6	11
25	Diffusion along interphase boundaries and its effect on retrograde zoning patterns of metamorphic minerals. Contributions To Mineralogy and Petrology, 2007, 154, 205-216.	1.2	15
26	Enhanced mass transfer through short-circuit diffusion: Growth of garnet reaction rims at eclogite facies conditions. American Mineralogist, 2006, 91, 1024-1038.	0.9	54
27	Simplon fault zone in the western and central Alps: Mechanism of Neogene faulting and folding revisited. Geology, 2006, 34, 317.	2.0	25
28	Structural and metamorphic evolution of the Camughera – Moncucco, Antrona and Monte Rosa units southwest of the Simplon line,Western Alps. Eclogae Geologicae Helveticae, 2005, 98, 19-49.	0.6	59
29	Phase Relations and Chemical Composition of Phengite and Paragonite in Pelitic Schists During Decompression: a Case Study from the Monte Rosa Nappe and Camughera–Moncucco Unit, Western Alps. Journal of Petrology, 2005, 46, 2145-2166.	1.1	20
30	A Quaternary Solution Model for White Micas Based on Natural Coexisting Phengite–Paragonite Pairs. Journal of Petrology, 2005, 46, 2129-2144.	1.1	49
31	Deformation, mass transfer and mineral reactions in an eclogite facies shear zone in a polymetamorphic metapelite (Monte Rosa nappe, western Alps). Journal of Metamorphic Geology, 2004, 22, 97-118.	1.6	53
32	In-situ Shear Modulus Determination by Pressuremeter Tests in Opalinus Clay and Reconciliation with Laboratory Tests. Rock Mechanics and Rock Engineering, 0, , .	2.6	0